EUROPEAN ORGANIZATION FOR NUCLEAR RESEARCH

1 July 97

Antiproton-proton annihilation at rest into $K_L K_S \pi^0 \pi^0$

A. Abele[8], J. Adomeit[7], C. Amsler[15], C.A. Baker[5], B.M. Barnett[3], C.J. Batty[5], M. Benayoun[12], A. Berdoz[13], K. Beuchert[2], S. Bischoff[8] P. Blüm[8], K. Braune[11], D.V. Bugg[9], T. Case[1], O. Cramer[11], V. Credé[3], K.M. Crowe[1], T. Degener[2], N. Djaoshvili[8], S. v. Dombrowski[15,a], M. Doser[6], W. Dünnweber[11], A. Ehmanns[3], D. Engelhardt[8], M.A. Faessler[11], C. Felix[11,b], P. Giarritta[15], R.P. Haddock[10], F.H. Heinsius[1,c], M. Heinzelmann[15], M. Herz[3], N.P. Hessey[11], P. Hidas[4], C. Hodd[9], C. Holtzhaußen[8] D. Jamnik[11,d], H. Kalinowsky[3], B. Kämmle[7], P. Kammel[1], J. Kisiel[6,e], E. Klempt[3], H. Koch[2], C. Kolo[11], M. Kunze[2], U. Kurilla[2], M. Lakata[1], R. Landua[6], H. Matthäy[2], R. McCrady[13], J. Meier[7], C.A. Meyer[13], L. Montanet[6], R. Ouared[6], F. Ould-Saada[15], K. Peters[2], B. Pick[3], C. Pietra[15], C.N. Pinder[5], M. Ratajcak[2], C. Regenfus[11], J. Reißmann[7], S. Resag[3], W. Roethel[11], P. Schmidt[7], I. Scott[9], R. Seibert[7], S. Spanier[15], H. Stöck[2], C. Straßburger[3], U. Strohbusch[7], M. Suffert[14], U. Thoma[3], M. Tischhäuser[8], C. Völcker[11], S. Wallis[11] D. Walther[11,f], U. Wiedner[11], B.S. Zou[9], and Č. Zupančič[11]

Crystal Barrel Collaboration

Abstract

The annihilation channel $\bar{p}p \rightarrow K_L K_S \pi^0 \pi^0$ was studied with the Crystal Barrel detector at LEAR. This final state with negative C-parity is dominated by the strange resonances $K^*(892)$, $K_1(1270)$, $K_1(1400)$ and $K_0^*(1430)$. In addition, a $J^{PC} = 1^{+-}$ state is seen in the K^*K decay mode. This state could be the isoscalar, axialvector h_1' seen here with a mass of $m = (1440 \pm 60)\,\mathrm{MeV}/c^2$ and a width of $\Gamma = (170 \pm 80)\,\mathrm{MeV}/c^2$.

This is the first experimental study and partial wave analysis of the $K_L K_S \pi^0 \pi^0$ final state produced in $\bar{p}p$ annihilation at rest. The same final state has previously been indirectly identified in the reaction $\bar{p}p \to K_S M$ by Astier *et al.* [1], where M represents the missing neutral particle system $K_L \pi^0 \pi^0$. With three missing particles, no partial wave analysis could be performed. However, an amplitude analysis of the related reaction $\bar{p}p \to K_S K_S \pi^+ \pi^-$ was possible and was found to be dominated by $K_1(1270)$ production in the decay mode $K_1(1270) \to K\rho$. It turns out that the reaction $\bar{p}p \to K_L K_S \pi^0 \pi^0$ is dominated by $K_1(1400)$ production in the decay mode $K^* \pi$.

The $K_L K_S \pi^0 \pi^0$ final state is also well suited to search for resonances decaying to $K_L K_S \pi^0$, via $K^* K$ or $\phi \pi^0$. The $K\bar{K}\pi$ sub-system has been studied extensively for 30 years and has revealed the presence of several resonances in the 1400–1500 MeV/c^2 mass region. It has mostly been studied in its $K_S K^\pm \pi^\mp$ combination, which can have positive or negative charge parity $C = \pm 1$. In radiative J/ψ decays or $\gamma\gamma$ interactions it can only be produced with $C = +1$. In the present study, the $K\bar{K}\pi$ system is observed as $K_L K_S \pi^0$ and is therefore in a pure $C = -1$ state. This clean environment allows further investigation of poorly known states, like the $J^{PC} = 1^{--}$ $\rho(1450) \to \phi\pi$[2] and the strangeonium of the 1^{+-} nonet, the $h_1(1380) \to K^* K$ [3].

The experiment was performed with the Crystal Barrel detector [4], exposed to a low momentum $\bar{p}$ beam from the Low Energy Antiproton Ring (LEAR) at CERN. The detector was designed to study exclusive final states where all charged and all neutral particles in an event are reconstructed. Antiprotons with a momentum of 200 MeV/c are stopped in a liquid hydrogen target at the centre of the detector. A five-fold segmented silicon counter in front of the target defines the incoming $\bar{p}$ beam and the level zero trigger. The target is surrounded by two cylindrical proportional wire chambers (PWCs) which give a fast level one trigger on the charged multiplicity which is required to be zero. This trigger selects with high efficiency all-neutral events, e.g. events with only photons in the final state. The wire chambers are surrounded by a cylindrical jet-drift chamber (JDC) and a barrel-shaped electromagnetic calorimeter of 1380 CsI(Tl) crystals. The 16 radiation lengths deep crystals are read out by wavelength shifters, coupled to photodiodes. They

1) University of California, LBL, Berkeley, CA 94720, USA
2) Universität Bochum, D-44780 Bochum, Germany
3) Universität Bonn, D-53115 Bonn, Germany
4) Academy of Science, H-1525 Budapest, Hungary
5) Rutherford Appleton Laboratory, Chilton, Didcot OX11 0QX, UK
6) CERN, CH-1211 Genève 23, Switzerland
7) Universität Hamburg, D-22761 Hamburg, Germany
8) Universität Karlsruhe, D-76021 Karlsruhe, Germany
9) Queen Mary and Westfield College, London E1 4NS, UK
10) University of California, Los Angeles, CA 90024, USA
11) Universität München, D-80333 München, Germany
12) LPNHE Paris VI, VII, F-75252 Paris, France
13) Carnegie Mellon University, Pittsburgh, PA 15213, USA
14) Centre de Recherches Nucléaires, F-67037 Strasbourg, France
15) Universität Zürich, CH-8057 Zürich, Switzerland
a) Now at Cornell University, Cornell, Ithaka, NY, USA
b) This work is part of a forthcoming Ph.D. thesis of C. Felix
c) Now at Universität Freiburg, Freiburg, Germany
d) University of Ljubljana, Ljubljana, Slovenia
e) University of Silesia, Katowice, Poland
f) Now at Universität Bonn, Bonn, Germany

cover 95% of 4π sr and provide an energy resolution of $\sigma_E/E \simeq 2.5\%/\sqrt[4]{E[\,\mathrm{GeV}]}$ and a typical angular resolution of $\sim 20\,\mathrm{mr}$ in both polar and azimuthal angles. All detectors are located in a homogeneous magnetic field of 1.5 T parallel to the incident $\bar{\mathrm{p}}$ beam.

The hermeticity of the Crystal Barrel detector and the high efficiency in the detection of low energy photons allows the study of the $\mathrm{K_L K_S}\pi^0\pi^0$ final state in its all-neutral decay mode:

$$\bar{\mathrm{p}}\mathrm{p} \to \mathrm{K_L^{missing}}\,\mathrm{K_S}\,\pi^0\,\pi^0$$

$$\pi^0 \to \gamma\gamma, \quad \pi^0 \to \gamma\gamma$$

$$\mathrm{K_S} \to \pi^0\pi^0, \quad \pi^0 \to \gamma\gamma, \quad \pi^0 \to \gamma\gamma$$

The $\mathrm{K_L}$ is required not to decay nor interact within the detector and is identified by missing momentum and energy in an otherwise complete event. The $\mathrm{K_L^{missing}K_S}\pi^0\pi^0$ final state is selected from $\sim 17\times 10^6$ triggered all-neutral events. First, events with residual tracks in the drift chamber are removed. Such events can be caused by small inefficiencies of the proportional wire chambers, by γ conversions in the drift chamber itself and by $\mathrm{K_S} \to \pi^+\pi^-$ decays outside the PWCs. From the resulting clean all-neutral sample, events with exactly eight isolated electromagnetic showers with a minimum energy deposit of 20 MeV in the crystals are selected. Events with a missing $\mathrm{K_L}$ are preselected by cutting on the total energy deposit E_{tot}

$$970\,\mathrm{MeV} < E_{tot} = \sum_{i=1}^{8} E_i^{shower} < 1450\,\mathrm{MeV}.$$

The edge crystals, $\theta < 18°$ and $\theta > 162°$, are not considered part of the fiducial volume if they contain the centre, i.e. the maximum energy deposit, of an electromagnetic shower. Those events are likely to have a large missing energy and are rejected. The direction of the measured momentum of an event must lie within $21° < \theta < 159°$. This ensures that the missing momentum of the non-interacting $\mathrm{K_L}$ points to a sensitive detector region. These cuts leave 9.7×10^4 events for further analysis. The purity of the data sample at this stage is shown in Fig. 1 for events, where the 8 electromagnetic showers (photons) can be combined to 4 π^0, which is possible for about 2×10^4 events. A clear $\mathrm{K_L}$ peak can be seen in the missing mass spectrum of Fig. 1a. The companion $\mathrm{K_S}$ is shown in its $\pi^0\pi^0$ decay mode in Fig. 1b, where an additional cut on the missing mass of the event was made, $400\,\mathrm{MeV}/c^2 < m_{miss} < 600\,\mathrm{MeV}/c^2$, selecting $\mathrm{K_L}$ and leaving about 13×10^3 events.

The following analysis returns to the above mentioned 9.7×10^4 events and only the missing mass cut is applied, which is mainly for the benefit of the kinematic fitting program, which has then to cope with fewer events. This cut leaves 44608 events as input to the kinematic fit. The first hypothesis is a one-constraint (1C) fit to the reaction $\bar{\mathrm{p}}\mathrm{p}\to 8\gamma\mathrm{K_L^{missing}}$ and fulfilled by 37230 events at a confidence level (CL) larger than 1%. The next step is a 6C fit to the hypothesis $\bar{\mathrm{p}}\mathrm{p}\to\mathrm{K_L^{missing}K_S}\pi^0\pi^0$ which yields 11542 events with CL>1%, and in the last step, events also fitting $\mathrm{K_L^{missing}}\eta\pi^0\pi^0\pi^0$ are discarded. The final sample consists of 7434 events with CL>10% for the hypothesis $\bar{\mathrm{p}}\mathrm{p}\to\mathrm{K_L^{missing}K_S}\pi^0\pi^0$. The background channel $\bar{\mathrm{p}}\mathrm{p} \to \mathrm{K_S K_S}\pi^0\pi^0$ with positive C-parity was investigated with a Monte-Carlo simulation based on GEANT3 [5] and found to be negligible. The overall efficiency to reconstruct and identify the reaction $\bar{\mathrm{p}}\mathrm{p}\to\mathrm{K_L K_S}\pi^0\pi^0$ in the all-neutral decay modes with a missing $\mathrm{K_L}$ was determined from the simulation to be $\epsilon = (13\pm 1)\%$, which means that only 3.9% of the produced $K_LK_S\pi^0\pi^0$ events are fully reconstructed. The probability, that the K_L does not interact in the crystals is $(46 \pm 4)\%$ which results in a branching ratio for this reaction of $BR(\bar{p}p\to K_LK_S\pi^0\pi^0) = (1.1 \pm 0.2)\times 10^{-3}$.

The general features of the $K_LK_S\pi^0\pi^0$ final state are displayed in Fig. 2, where a clear ϕ signal can be seen in the invariant K_LK_S mass spectrum as well as two strong $K^*(892)$ bands in the $m^2(K_L\pi^0)$ versus $m^2(K_S\pi^0)$ scatterplot. Already at this initial step of the analysis the 2-body K^*K^* and the 3-body $\phi\pi^0\pi^0$ final states are clearly visible. Most events contain at least one K^* and therefore the 4-body final state can be reduced to the 3-body final state $K^*K\pi^0$ which is suited for a Dalitz plot analysis. The K^* events are selected by a K^* mass cut, $0.74\,\mathrm{GeV}^2/c^4 < m^2_{K\pi} < 0.84\,\mathrm{GeV}^2/c^4$, and the Dalitz plot with projection is shown in Fig. 3. The two main features are indicated by arrows: a strong horizontal K^* band and a faint vertical band at a K^*K invariant mass around $1.4\,\mathrm{GeV}/c^2$. This band could be caused by a resonance with negative C-parity and isospin $I=0$ or 1 decaying into K^*K. However, it could also contain reflections from strange resonances decaying into $K\pi\pi$.

Therefore a partial wave analysis of the $K_LK_S\pi^0\pi^0$ final state in the full 5-dimensional space of kinematic variables was performed. It is assumed that the initial $\bar{p}p$ system reaches the $K_LK_S\pi^0\pi^0$ final state through a series of quasi two-body decays. The angular dependences of the transition amplitudes $\mathcal{A}_i$ are constructed in the helicity formalism [7, 8]; relativistic Breit-Wigner functions with an energy dependent width and Blatt-Weisskopf penetration factors [9] describe the dynamics of the intermediate two-body resonances. For a J^{PC}=0^{++} $(\pi^0\pi^0)$ intermediate state, subsequently designated by $(\pi\pi)_S$, the Breit-Wigner function is replaced by the $\pi\pi$ S-wave [10]. Explicit expressions for these amplitudes are given in Reference [11]. Similarly, for a J^{PC}=0^{++} $(K^0\pi^0)$ intermediate state, subsequently designated by $(K\pi)_S$, the Breit-Wigner function is replaced by the $K\pi$ S-wave given in Reference [12].

The quantum numbers of the initial $\bar{p}p$ state are restricted by C-parity conservation. The annihilation into the $K_LK_S\pi^0\pi^0$ final state can occur only from the $^3S_1$ $(J^{PC}=1^{--})$ or the $^1P_1$ $(J^{PC}=1^{+-})$ $\bar{p}p$ atomic orbitals (initial states with higher orbital angular momentum do not contribute to $\bar{p}p$ annihilation at rest). Initially, only annihilation from 1^{--} will be considered. A minimal set of amplitudes, containing only well established intermediate states, is as follows:

1. $\bar{p}p\to(K\pi)_SK^*(892)$, relative angular momentum $L=0$
2. $\bar{p}p\to K^*(892)\bar{K}^*(892)$, $L=1$, total spin $S=0$ or $S=2$
3. $\bar{p}p\to K_1(1270)K^0$, $L=0$
   Four decay modes of the $K_1(1270)$ are considered:
   (a) $K_1\to K^*(892)\pi$, $L=0$
   (b) $K_1\to K^*(892)\pi$, $L=2$
   (c) $K_1\to(K\pi)_S\pi$, $L=1$
   (d) $K_1\to K(\pi\pi)_S$, $L=1$
4. $\bar{p}p\to K_1(1400)K^0$, $L=0$
   The same four decay modes as for $K_1(1270)$ are also considered for $K_1(1400)$.
5. $\bar{p}p\to\phi(\pi\pi)_S$, $L=0$
6. Incoherent background amplitude, i.e. $K_LK_S\pi^0\pi^0$ phase space.

The masses and widths of all particles have their PDG values [14] and are fixed in the fits, except when mentioned explicitly.

The data are subjected to a maximum likelihood fit using the MINUIT [15] minimization package. The likelihood function $\mathcal{L}$ is constructed from a coherent sum of the transition amplitudes $\mathcal{A}_i$

$$\mathcal{L} = \prod_k \frac{|\sum_i \alpha_i \mathcal{A}_i|^2 + \mathcal{B}}{\int |\sum_i \alpha_i \mathcal{A}_i|^2 \epsilon(\Omega) d\Omega + \mathcal{B}} ,$$

where α_i are complex fitting parameters while $\mathcal{B}$ is a positive parameter representing an assumed incoherent background, uniformly distributed in phase space. The product runs over all experimental events, in this case $k = 1 \cdots 7434$. The normalization integral is calculated with Monte Carlo events which had to pass the same acceptance cuts (represented by $\epsilon(\Omega)$) as the experimental data.

A fit with the minimal set of amplitudes and pure initial S-wave annihilation gives a fairly good description of the experimental data. Since the channels containing $K_1(1270)$ decays contribute very litte, only the channel (3a) was taken into account. Starting from this fit, a search for less well established or unknown particles produced from the 1^{--} state and decaying to $\phi\pi^0$, $K^*\pi^0$ or K^*K was performed.

A $J^{PC} = 1^{--}$ resonance $X \to \phi\pi^0$ with a width of $150\,\mathrm{MeV}/c^2$, scanned through the mass range between 1200 and $1700\,\mathrm{MeV}/c^2$, produces a maximum increase in log-likelihood of $\Delta ln\mathcal{L} = 15$ for a mass of $m_X \approx 1500\,\mathrm{MeV}/c^2$ with less than 50 events attributed to it. Resonances $X \to K^*\pi^0$ with $J^P = 0^-$ ($\Gamma = 260\,\mathrm{MeV}/c^2$), 1^- ($\Gamma = 230\,\mathrm{MeV}/c^2$) and 2^+ ($\Gamma = 110\,\mathrm{MeV}/c^2$), scanned through the mass range 1200 to $1750\,\mathrm{MeV}/c^2$ give at best $\Delta ln\mathcal{L} = 19$ for a 2^+ state with mass $m_X \approx 1400\,\mathrm{MeV}/c^2$, but again less than 50 events. These indications of weak contributions of additional intermediate resonances are not sufficiently significant to be included in further fits.

Next, the K^*K system was scanned for $J^{PC} = 1^{--}$ ($\Gamma = 150$ and $300\,\mathrm{MeV}/c^2$) and 2^{--} ($\Gamma = 200\,\mathrm{MeV}/c^2$) resonances. There are indications of 1^{--} states around $1400\,\mathrm{MeV}/c^2$ and just below $1700\,\mathrm{MeV}/c^2$, each with less than 100 events and of a 2^{--} state around $1600\,\mathrm{MeV}/c^2$ with less than 30 events. None of these intermediate states will be included in further fits.

The only substantial improvement over the minimal set of amplitudes is achieved by the addition of a $J^{PC} = 1^{+-}$ amplitude in the K^*K system around $1400\,\mathrm{MeV}/c^2$. Here, Aston et al. [3] have found a 1^{+-} state, called $h_1(1380)$ with $m = (1380 \pm 20)\,\mathrm{MeV}/c^2$ and $\Gamma = (80 \pm 30)\,\mathrm{MeV}/c^2$. A fit with these values gives a significant increase in log-likelihood by $\Delta ln\mathcal{L} = 42$. If mass and width are left free, log-likelihood reaches a maximum at $m = (1440 \pm 60)\,\mathrm{MeV}/c^2$ and $\Gamma = (170 \pm 80)\,\mathrm{MeV}/c^2$ with $\Delta ln\mathcal{L} = 126$. This mass is somewhat higher and the width larger than those of the $h_1(1380)$ found by Aston et al., although they agree within the experimental errors.

A summary of the rates and phases for the best fit with pure S-wave annihilation is given in Table 1 and a comparison of invariant mass distributions is shown in Figure 4. The intensity of the incoherent background is the fitted value $\mathcal{B}$ integrated over the available phase space, as it should be obtained in an experiment with 100% acceptance and expressed as a percentage of the total number of events. The analogous intensities of the individual amplitudes are normalized to add up to 100%, without the incoherent background. In order to calculate them, their interferences have been neglected. The phase angles of the fitted complex coefficients α_i are quoted separately. The contributions of some of the individual amplitudes are indicated in Figure 5.

The final results and errors, quoted in Table 1 include the variations observed for slightly different parametrizations of the amplitudes. For example, the energy dependent width in the Breit-Wigner function contains the nominal decay momentum q_0 of a resonance. This momentum is not well defined if one of the decay products is either the $\pi\pi$

Amplitude	Rate [%]	Phase [°]
$(\mathrm{K}\pi)_\mathrm{S}\mathrm{K}^*$, $L=0$	8 ± 3	0 fixed
$\mathrm{K}^*\bar{\mathrm{K}}^*$, $S=0$	5.2 ± 0.6	170 ± 10
$\mathrm{K}^*\bar{\mathrm{K}}^*$, $S=2$	3.5 ± 1	10 ± 10
$\mathrm{K}_1(1270)\mathrm{K}$ $\mathrm{K}_1(1270)\to\mathrm{K}^*\pi^0$, $L=0$	 4.6 ± 1	 135 ± 5
$\mathrm{K}_1(1400)\mathrm{K}$		
$\mathrm{K}_1(1400)\to\mathrm{K}^*\pi^0$, $L=0$	59 ± 3	70 ± 5
$\mathrm{K}_1(1400)\to\mathrm{K}^*\pi^0$, $L=2$	1.7 ± 0.6	65 ± 10
$\mathrm{K}_1(1400)\to(\mathrm{K}\pi)_\mathrm{S}\pi^0$, $L=1$	4 ± 1	55 ± 20
$\mathrm{K}_1(1400)\to\mathrm{K}(\pi\pi)_\mathrm{S}$, $L=1$	3 ± 1	50 ± 20
$\phi(\pi\pi)_\mathrm{S}$, $L=0$	3.0 ± 0.6	40 ± 5
$\mathrm{X}(1440)\pi^0$ $\mathrm{X}(1440)\to\mathrm{K}^*\mathrm{K}$, $L=0$ $m=1440\,\mathrm{MeV}/c^2, \Gamma=170\,\mathrm{MeV}/c^2$	 8 ± 4	 340 ± 5
Incoherent background	20 ± 5	

Table 1: Rates and phases of the main amplitudes contributing to the reaction $\bar{\mathrm{p}}\mathrm{p}\to\mathrm{K_L K_S}\pi^0\pi^0$. The normalization is such that the total intensity of all amplitudes minus background is 100%.

or $\mathrm{K}\pi$ S-wave. Different masses were tried and the fits were also done with an energy independent width Γ_0.

Furthermore, the same set of amplitudes was used in fits with $\bar{\mathrm{p}}\mathrm{p}$ annihilation from initial S- and P-waves ($^3\mathrm{S}_1$, $^1\mathrm{P}_1$). The log-likelihood increases by ≈ 30, but the number of free parameters is almost twice as large as for the S-wave fit only. The P-wave contribution varies between 10 to 20% and the total contributions of the individual amplitudes change very little.

It is remarkable that the $\mathrm{K}_1(1400)\mathrm{K}^0$ final state has a phase which is nearly independent of the $\mathrm{K}_1(1400)$ decay mode and that the relative phase between the two $\mathrm{K}^*\bar{\mathrm{K}}^*$ contributions with total spin $S=0$, resp. $S=2$ is about 180°. Even more remarkable is the dominance of the $\mathrm{K}_1(1400)$ and the weakness of the $\mathrm{K}_1(1270)$.

It is interesting to compare the results of the present work with those of Abele et al. [17] on the related annihilation channel $\mathrm{K_L K}^\pm\pi^\mp\pi^0$, keeping in mind that this channel receives contributions also from initial states with positive C-parity. The relative ratio of $\mathrm{K}_1(1400)$ over $\mathrm{K}_1(1270)$ production should be the same in both reactions. However, $\mathrm{K}_1(1270)$ production is almost negligible in $\mathrm{K_L K_S}\pi^0\pi^0$, whereas it is large in $\mathrm{K_L K}^\pm\pi^\mp\pi^0$, about 50% of $\mathrm{K}_1(1400)$. This could be understood, if $\mathrm{K}_1(1270)$ decayed dominantly into $\mathrm{K}\rho$ which cannot be observed in $\mathrm{K_L K_S}\pi^0\pi^0$. However, this explanation is in contradiction to the $\mathrm{K_L K}^\pm\pi^\mp\pi^0$ analysis, where roughly equal decay probabilities of $\mathrm{K}_1(1270)$ into $\mathrm{K}\rho$ and $\mathrm{K}^*\pi$ were found.

Another important comparison concerns the X(1440) intermediate state. Qualitatively, the $\mathrm{K_L K_S}\pi^0$ invariant mass spectrum (Fig. 4d) exhibits a considerably steeper increase of intensity around $1400\,\mathrm{MeV}/c^2$ than the $\mathrm{K_L K}^\pm\pi^\mp$ spectrum (Fig. 2 in Ref. [17]). This is the expected behaviour for a relatively larger contribution of the X(1440) resonance in the $\mathrm{K_L K_S}\pi^0\pi^0$ channel as compared to $\mathrm{K_L K}^\pm\pi^\mp\pi^0$. If X(1440) were an isolated resonance, its branching ratio into $\mathrm{K_L K}^\pm\pi^\mp$ should be twice that for the decay into $\mathrm{K_L K_S}\pi^0$.

In that case one could conclude from the branching ratio of 9.3×10^{-4} for $\bar{p}p\to K_L K_S \pi^0\pi^0$, 8% of which proceeds through $X(1440)\pi^0$, that about 360 $X(1440)\to K_L K^\pm\pi^\mp$ events should be observed in the $K_L K^\pm\pi^\mp\pi^0$ channel. Substantial deviations from this prediction could be caused by interferences with other intermediate states in that channel. In the $K_L K^\pm\pi^\mp$ spectrum of Ref. [17] an excess of about 200 events is visible above the fit around 1440 MeV/c^2. Since the fit does not include any $K_L K^\pm\pi^\mp$ resonance, it is to be expected that it passes below the peak but above the tails of a narrow $K_L K^\pm\pi^\mp$ resonance. Different exploratory fits trying to include such a resonance favoured $J^P=1^+$ for its quantum numbers and yielded intensities from about 200 to 800 events, clearly not contradicting the above naive prediction. Within errors, the position and width of this resonance were in accord with the values found in the present work.

However, in the partial wave analysis of the $K_L K^\pm\pi^\mp\pi^0$ channel, a coherent contribution of X(1440) to the $^3S_1$ amplitude was not favoured. Instead, the additional events could be better explained by an incoherent source, such as $f_1(1420)$ accessible in P-wave annihilation. In view of the small relative number of the surplus events around 1440 MeV/c^2 in the $K_L K^\pm\pi^\mp$ spectrum and the general difficulties with small amplitudes and P-wave annihilation in partial wave analyses, one cannot at present draw any definitive conclusion on the manifestation of X(1440) in the channel $K_L K^\pm\pi^\mp\pi^0$.

In summary, the reaction $\bar{p}p\to K_L K_S\pi^0\pi^0$ can be described by the well known strange resonances $K^*(892)$, $K_1(1270)$, $K_1(1400)$ and the $K\pi$ S-wave, the $\phi(1020)$ and a state with quantum numbers $J^{PC}=1^{+-}$. This state has a mass of $m=(1440\pm60)$ MeV/c^2, a width of $\Gamma=(170\pm80)$ MeV/c^2, and decays dominantly to K^*K. The only other experimental evidence for this state comes from the LASS experiment where a slightly lower mass (1380 ± 20 MeV/c^2) and a narrower width (80 ± 30 MeV/c^2) were obtained [3]. However, both measurements agree within their errors. This particle could be the *strangeonium* of the axial vector nonet, the h_1'. If the masses of the members of this nonet are compared with the well established particles of the tensor (2^{++}) nonet, the 1^{+-} strangeonium would be expected about to lie 100 MeV/c^2 below the $f_2'(1525)$, very close to our measurement of $m=1440$ MeV/c^2.

Acknowledgements

We would like to thank the technical staff of the LEAR machine group and of all the participating institutions for their invaluable contributions to the success of the experiment. We acknowledge financial support the German Bundesministerium für Bildung, Wissenschaft, Forschung und Technologie, the Schweizerischer Nationalfonds, the British Particle Physics and Astronomy Research Council, the U.S. Department of Energy and the National Science Research Fund Committee of Hungary (contract No. DE–FG03–87ER40323, DE–AC03–76SF00098, DE–FG02-87ER40315 and OTKA F014357). K. M. C., N. D. and F. H. H. acknowledge support from the Alexander von Humboldt Foundation.

References

[1] A. Astier et al., *Nucl. Phys.* B10(1969)65.
[2] S. I. Bityukov et al., *Phys. Lett.* B188(1987)383.
[3] D. Aston, *Phys. Lett.* B201(1988)573.
[4] E. Aker et al., *Nucl. Instr. Methods* A321(1992)69.
[5] R. Brun et al., GEANT3, Internal Report CERN DD/EE/84-1 (1986).
[6] C. Amsler et al., *Phys. Lett.* B346(1995)364.

[7] M. Jacob and G. C. Wick, *Ann. Phys. (N.Y.)* 7(1959)404.
[8] C. Amsler and J. C. Bizot, *Comp. Phys. Comm.* 30(1983)21.
[9] J.M. Blatt and V.F. Weisskopf, *Theoretical Nuclear Physics*, Wiley, New York 1952.
F. von Hippel and C. Quigg, *Phys. Rev.* D5(1972)624.
[10] K. L. Au et al., *Phys. Rev.* D35(1987)1633.
[11] C. Amsler et al., *Phys. Lett.* B311(1993)362.
[12] C. Amsler et al., *Phys. Lett.* B385(1996)425.
[13] D. Aston, *Nucl. Phys.* B296(1988)493.
[14] Review of Particle Physics, *Phys. Rev.* D54(1996).
[15] CERN Program Library Entry D506, MINUIT, Version 92.1 (1992).
[16] C. Daum et al., *Nucl. Phys.* B187(1981)1.
[17] A. Abele et al., accompanying letter.

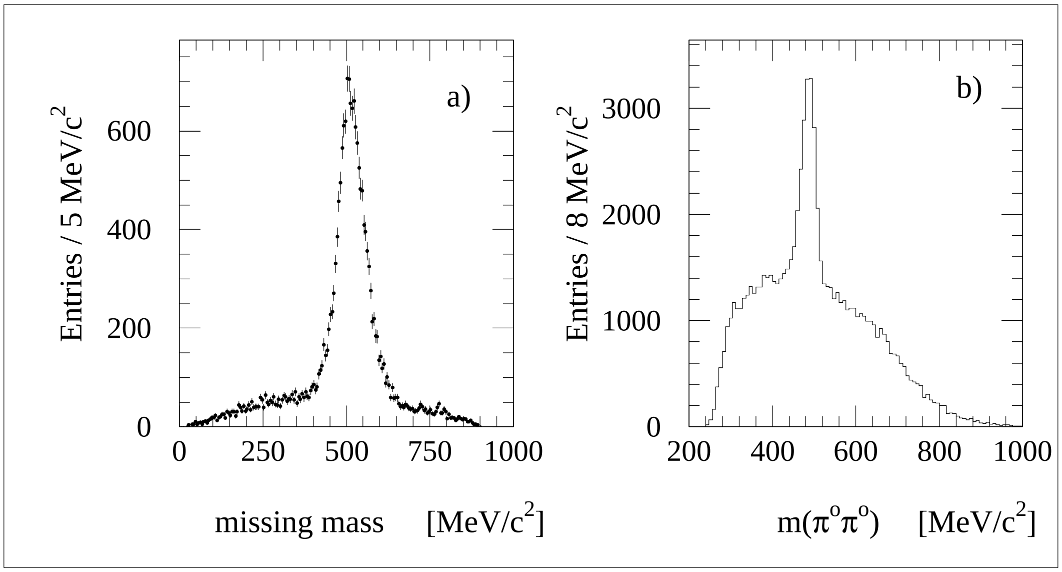

Figure 1: Missing mass and invariant mass distributions after the cuts described in the text; a) Missing mass spectrum for 4 π^0 events showing the non-interacting K_L; b) Invariant $\pi^0\pi^0$ mass showing the K_S peak on top of a mainly combinatorial background (6 entries per event).

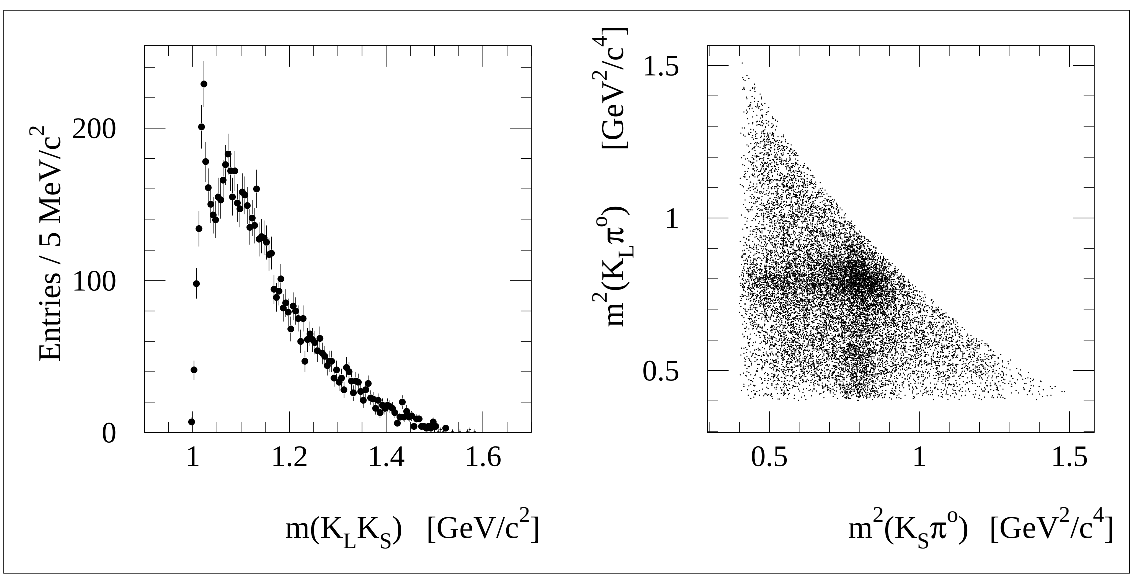

Figure 2: The K_LK_S invariant mass distribution (left) and the $K\pi^0$ scatter plot (right, 2 entries per event) show the ϕ and $K^*(892)$ contributions to the $K_LK_S\pi^0\pi^0$ final state.

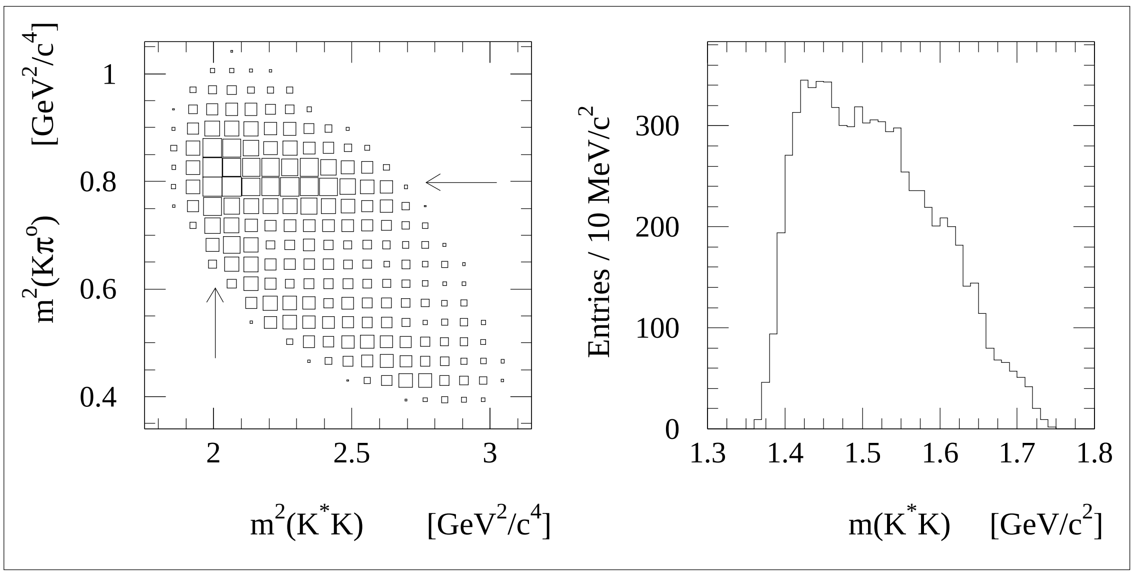

Figure 3: The $K^*K\pi^0$ Dalitz plot and its K^*K projection. There are up to four entries per event, depending on the number of good K^* combinations.

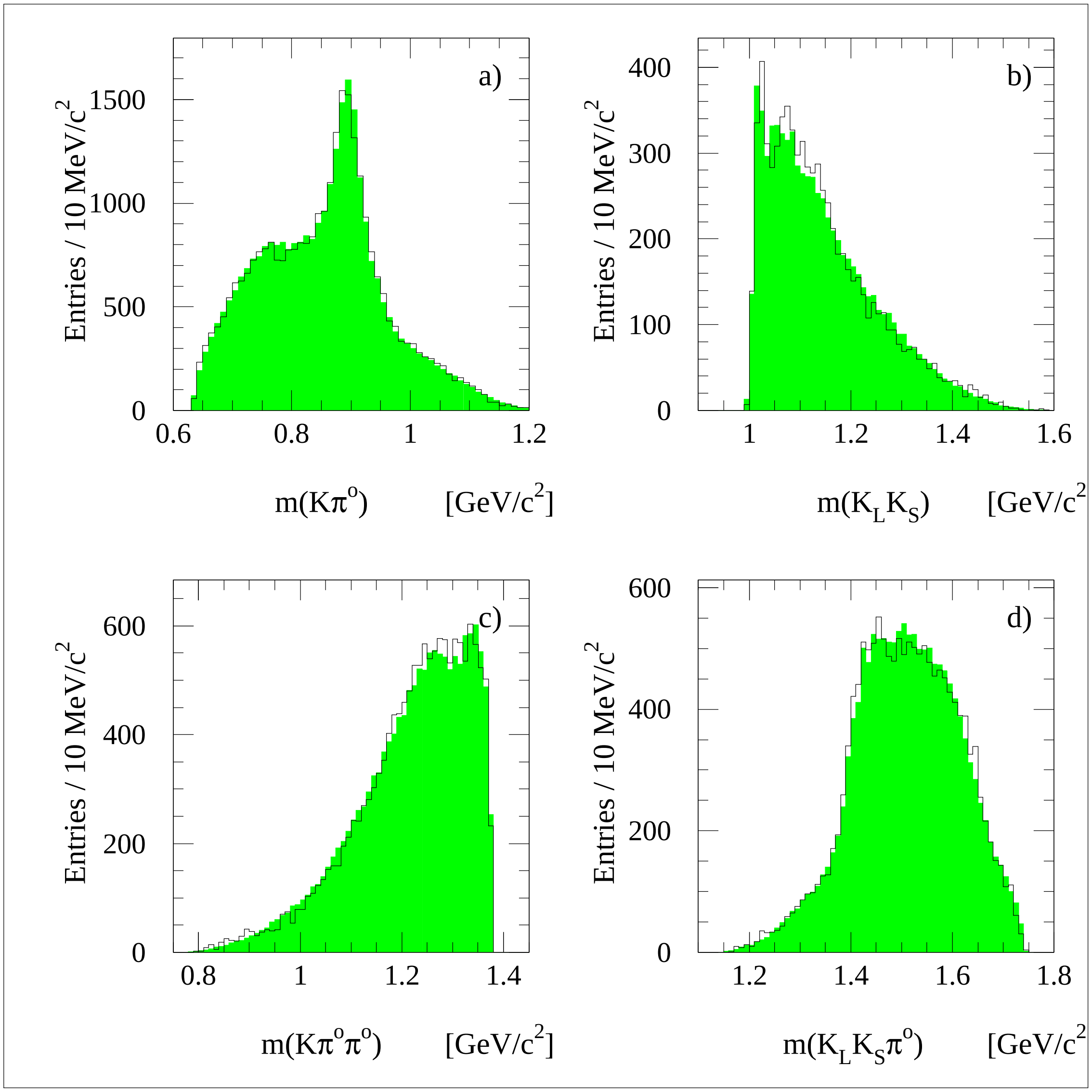

Figure 4: Two and three particle invariant mass distributions. The fit is represented by the shaded area: a) $K\pi^0$ invariant mass (4 entries per event); b) K_LK_S invariant mass (1 entry per event); c) $K\pi^0\pi^0$ invariant mass (2 entries per event); d) $K_LK_S\pi^0$ invariant mass (2 entries per event).

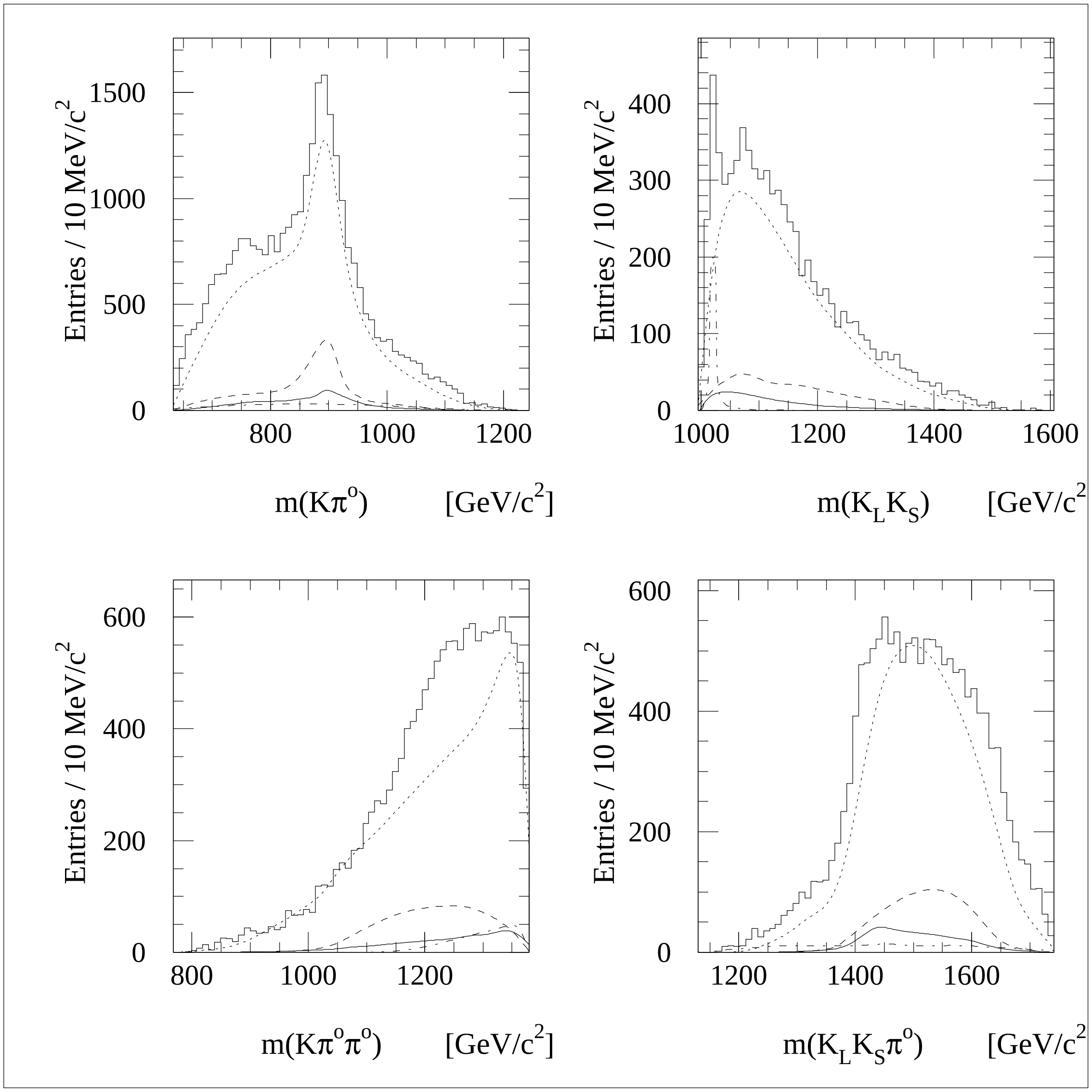

Figure 5: Two and three particle invariant mass distributions with contributions from some amplitudes. The data are represented by the histogram and the amplitudes are indicated by smooth lines; dashed: $K^*\bar{K}^*$, dotted: $K_1(1400)$, dashed-dotted: $\phi(\pi\pi)_S$ and full: $h_1(1440)$.